The final publication is available at

https://doi.org/10.1016/j.polymdegradstab.2017.06.004

Additional Information

Relevant factors for the eco-design of polylactide/sisal biocomposites to control biodegradation in soil in an end-of-life scenario

J. D. Badia[1,2], E. Strömberg[3], T. Kittikorn[3,4], M. Ek[3], S. Karlsson[3], A. Ribes-Greus[1,*]

Abstract

The eco-design considers the factors to prepare biocomposites under an end-of-life scenario. PLA/sisal biocomposites were obtained from amorphous polylactide and sisal loadings of 10, 20 and 30 wt% with and without coupling agent, and subjected to biodegradation in soil according to standard ISO846. Mass-loss, differential scanning calorimetry and size-exclusion chromatography were used for monitoring biodegradation. A statistical factorial analysis based on the molar mass M_n and crystallinity degree X_C pointed out the relevance and interaction of amount of fibre and use of coupling agent with the time of burial in soil. During the preparation of biocomposites, chain scission provoked a similar reduction of M_n for coupled and non-coupled biocomposites. The amount of fibre was relevant for the increase of X_C due to the increase of nucleation sites. The coupling agent accelerated the evolution of both factors: reduction of M_n and the consequent increase of X_C, mainly during biodegradation in soil. Both factors should be balanced to facilitate microbial assimilation of polymer segments, since bacterial digestion is enhanced by chain scission but blocked by the promotion of crystalline fractions.

Keywords

Polylactide (PLA); natural fibre; sisal; biocomposite; degradation; biodegradation in soil; design of experiments; statistical factorial analysis; size exclusion chromatography; differential scanning calorimetry;

Highlights

- Eco-design considered fibre and coupling agent in an end-of-life scenario
- Statistic relevance and interaction of sisal and coupling agent during burial in soil
- Sisal induced increase of nucleation sites for crystalline fraction
- Coupling agent accelerated chain scission and formation of crystallites
- Biodegradation mainly affected PLA/sisal biocomposites with coupling agent

Graphical abstract
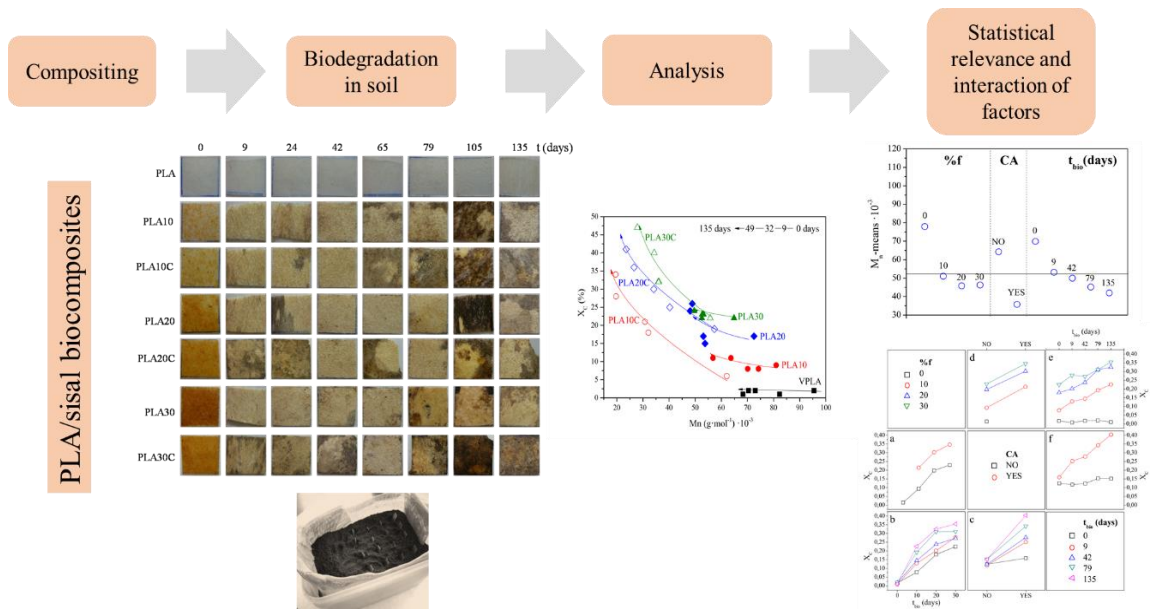
1. Introduction

The use of bio-based composites based on renewable polymer matrixes and natural fibres as alternative materials are continuously increasing in several applications such as packaging or household and agricultural equipment [1]–[3]. The eco-design of plastic materials from renewable resources for high-consume applications such as packaging or agricultural mulches moves towards the design of sustainable polymers with controlled degradability and enhanced bio-reintegration. Cradle-to-cradle design enables the establishment of completely beneficial industrial systems driven by the synergistic search of positive economic, environmental and social goals [4].

The use of sisal [5] has been reported for biopolymers such as polylactide [6]–[8], poly(hydroxyl butyrate-co-valerate) [9], [10], starch-based matrixes [11]–[13] or chitosan [14]. Natural fibres such as sisal present low densities, low cost, non-abrasive nature, high filling level, low energy consumption, high specific properties, biodegradability, etc., over synthetic fibres. However, the absorption of moisture by untreated biofibres, poor wettability, and insufficient adhesion between the polymer matrix and fibre deteriorate the performance of the biocomposites. [15] In order to overcome the drawbacks, surface modifications of fibres [16] by means of processes such as esterification [17], silanization [17]–[19] or the use of maleic anhydride as coupling agent [20]–[22] are reported. Due to stability of biocomposites, there is a risk of wide scale environmental contamination and environmental issues similar to that seen with conventional plastics [23]. The balance of long-term properties of bio-based polymers and biocomposites is not usually connected to a proper end-of-life scenario [24]. Actually, most of them retain their properties after their service life and are uncontrolledly discarded [25], which could be approachable by means of burial in soil, that might induce biodegradation.

In order to understand and control the biodegradation state of these materials after disposal, several standards can be followed [26]. The use of the ISO846 [27], consisting in burial in active soil at 28ºC and controlled humidity is feasible to simulate the uncontrolled disposal of polymers, has been shown for polylactide [28]–[30], polyurethane [31], silicon rubber [32] or plasticised starch [33]. The biodegradation rate in this norm is usually followed by mass-loss after the disintegration state, which seldom represents a proper indicator to monitor biodegradation [30]. Indeed, before disintegration, the materials undergo structural and morphological modifications that are

4

not assessable by the methods foreseen in the standard. Therefore, specific techniques such as size-exclusion chromatography and differential scanning calorimetry offer a fast and cost-reliable alternative to monitor the degradation state of biopolymers and biocomposites [24]. It is well-stated that degradation induces chain scission, which may ease the assimilation of oligomeric species by microorganisms in soil. However, it is also well-known that degradation mainly takes place in the amorphous fraction of polymers and therefore the formation of crystalline phase may difficult the chain scission and ulterior incorporation into the C-cycle by microorganisms. Therefore, the monitoring of both the molar mass and the degree of crystallinity may help interpret the biodegradation profile of biocomposites according to the balance between both competitive processes. Indeed, the abiotic and biotic environmental degradation of the bioplastics such as polylactide is reported [34], but it becomes more complex when other factors such as the amount of fibre and coupling agent in biocomposites are taken into account [35].

Summing up, the design of biocomposites is performance-focused, and therefore the addition of certain fibres and the improvement of the interfaces to achieve certain mechanical specifications are usually pursued. However, the eco-design of the same biocomposites should also consider the impact of these factors once the service life has been fulfilled, under an end-of-life scenario. In this work, PLA/sisal biocomposites were therefore prepared from amorphous polylactide and sisal loadings of 10, 20 and 30 wt% with and without coupling agent, and subjected to biodegradation in soil according to standard ISO846. The eco-design factors under study were the amount of fibre and the use of coupling agent. The variable of monitoring biodegradation was the time if burial. The effects under consideration were the molar mass, as obtained from size exclusion chromatography, and the crystallinity degree and thermal properties, as obtained by differential scanning calorimetry. The aim was to qualitatively assess the correlation between molar mass and crystallinity degree during biodegradation in soil before disintegration. The use of a statistical factorial analysis [36] to understand the relevance and possible interaction of the factors under study was used to shed more light on the understanding of the effects of biodegradation in soil on the biocomposites.

5

2. Experimental procedure

2.1. Materials and reagents

Polylactide (PLA) 3251D was purchased from Natureworks (Minnetonka, USA) as pellets with a glass transition in 65-70 ℃ range. Sisal fibres, a farming crop, were supplied by the Thai Royal Project [37]. Their length was about 0.5-1 mm, tensile strength of 550 MPa, tensile modulus of 30 GPa and density about 1.5 g/cm^3. Dicumyl peroxide (DCP) 98% (Sigma-Aldrich, Sweden AB) and maleic anhydride (MAH) M188-99% (Sigma-Aldrich, Sweden AB) were used as free radical initiator and coupling agent, respectively.

2.2. Preparation of PLA/sisal biocomposites

Prior to processing, neat PLA and sisal fibre were dried in an oven at 80 ℃ during at least 12 hours and kept in zip bags. The fibre contents in the biocomposite were formulated as 10%, 20% and 30% by weight with and without coupling agent. In case of not using MAH, the biocomposites were prepared in an internal mixer (Brabender, Germany) during 5 minutes at 180 ℃ and at the speed of 50 rpm. The resulting biocomposites were labelled as PLA10, PLA20 and PLA30. The biocomposites containing the coupling agent were prepared by incorporating MAH 2.5% and DCP 0.3% by weight in molten polymer and mixing during 5 minutes at 180 ℃ and at the speed of 50 rpm. These samples were labelled as PLA10C, PLA20C and PLA30C. The compounded PLA/sisal biocomposites were then ground and the granules dried at 80 ℃ in the oven during at least 12 h. The final 500 µm thick specimens were obtained by means of a compression moulding equipment (Fontijne Presses, Netherlands), by preheating the press to 200 ℃ for 2 min, and applying a compression force of 150 kN during 2 min under vacuum conditions. Finally, all compounded biocomposites were dried at 50 ℃ in a vacuum oven (Heraeus Vacutherm 6025, Germany), then kept in zip bags and placed in a desiccator for further analyses at normalized lab conditions according to ISO 291 [38].

2.3. Biodegradation in soil test

The PLA/sisal biocomposites were subjected to a controlled degradation in soil test under controlled conditions, following the ISO 846-1997 International Norm, method D [27] during 135 days. The specimens were buried in biologically active soil and kept in a Heraeus B12 (Hanau, Germany) culture oven at 28 ℃. The soil used in these tests was a red soil extract taken from a real agriculture field in Alginet (Valencia). The microbial

6

activity of soil was monitored with cotton along the extension of the experiment. The soil was maintained at approximately pH 7 and a relative humidity of 0.87 g water/g wet soil. To ensure the oxygenation of the soil, a protocol of periodical air oxygen supply was followed. Three specimens of each sample were extracted after certain times of burial in soil, cleaned and kept in a desiccator during 4 days in order to ensure water desorption before being analyzed.

2.4 Analytical characterisation

2.4.1. Mass-loss variance

The specimens of PLA/sisal biocomposites were weighed using a scale (Mettler Toledo AB135-S) with a precision of 0.1 mg. Three samples of each material were used to assess reproducibility.

2.4.2. Size Exclusion Chromatography (SEC)

The molar mass of PLA/sisal biocomposites was analysed by size exclusion chromatography (SEC). The samples were dissolved in chloroform (Fluka, purity of 99%) at 80 ℃ for 2 h. The sample solution was filtered for removal of contaminants and fibres before injecting the sample into the SEC column. The polymers were analysed with a Verotech PL-GPC 50 Plus system equipped with a PL-RI Detector and two PLgel 5 mm Mixed-D columns. The samples were injected by a PL-AS RT auto-sampler for PL-GPC 50 Plus, in which chloroform was used as mobile phase (1 mL·min^{-1}, 30 ℃). The calibration was created using polystyrene standards with a narrow molar mass distribution. Corrections for the flow rate fluctuations were performed using toluene as internal standard. Triplicates were performed to ensure reproducibility of results.

2.4.3. Differential Scanning Calorimetry (DSC)

DSC characterization of PLA/sisal biocomposites was carried out by a Mettler Toledo DSC 822 instrument (Columbus, OH) calibrated with indium and zinc standards. Approximately 5 mg of pellets were placed in 40 mL aluminium pans, which were sealed and pierced to allow the N_2 gas flow (50 mL·min^{-1}). A 10 ℃·min^{-1} heating rate was employed in the temperature range between 0 ℃ and 200 ℃. DSC analysis was performed with the aid of the software STAR^e 9.10 from Mettler-Toledo. The experiments were repeated at least thrice and the averages of temperatures and enthalpies were considered as representative.

7

2.5. Statistical factorial analysis

As shown in previous studies [39], [40], a statistical factorial analysis (SFA) involves the study of the influence of multiple factors on an experimental response [36], which can be either qualitative categorical variable, such as the use or not of coupling agent or quantitative based on discrete values of a quantifiable variable, such as the amount of fibre in the biocomposite. The variable of monitoring the time of biodegradation in soil was also included in the analysis as a factor. The effects chosen for the analysis were the molar mass, representative of chemical structure, and the crystallinity degree, representative of the physical morphology of the biocomposites. In particular, the SFA was performed according the group of factors and levels proposed in **Table 1**, with the aid of the Minitab® 15.1.0.0. software (Minitab Inc., USA).

Factor	Type	# levels	Value-level				Effect
Percentage of fibre (*%f, wt%*)	Quantitative	4	0	10	20	30	Molar mass (M_n)
Use of coupling agent (*CA*)	Qualitative	2	NO		YES		
Time of burial (t$_{bio}$, days)	Quantitative	5	0 9 42 79 135				Crystallinity degree (X_C)

Table 1. Summary of factors, levels and effects of the statistical factorial analysis performed in this study.

8

3. Results and discussion

The effects of biodegradation in soil of PLA/sisal biocomposites were initially assessed by mass loss, as stated in the normative. Afterwards, an in-depth analysis by size exclusion chromatography and differential scanning calorimetry permitted to monitor the structural and morphological variations, as well as thermal properties. The factors of design of the biocomposites under study were the amount of fibre and the use of coupling agent. The variable of monitoring biodegradation was the time of burial in soil. A statistical analysis helped understand the relevance and interaction of factors on the molar mass and the crystallinity degree. Finally, both parameters were correlated to picture the influence of the amount of fibre and the use of coupling agent on PLA/sisal biocomposites subjected to biodegradation in soil.

3.1. Monitoring of biodegradation in soil by the standard ISO846

The standard norm of biodegradation used in this study recommended the monitoring of biodegradation in terms of mass-loss, according to $n^{-1} \cdot \Sigma[(m_t - m_0) \cdot m_0^{-1}]$, being n the amount of specimens, m_t the mass at a time t and m_0 the initial mass of each sample. The values of the mass-loss are gathered for neat PLA and PLA/sisal biocomposites in **Figure 1**. Surprisingly, the values were positive and therefore did not represent mass-loss. Instead, a mass increase due to the absorption of water, as well as the low level of disintegration and inclusion of soil as shown in **Figure 2** This effect was more representative for those biocomposites with higher amount of sisal, due to the hydrophilic character of the fibres, which increased the kinetics and capability of water absorption [41], [42]. Accordingly, the measure of an eventual mass-loss was not representative enough to monitor the effects of biodegradation in soil on the PLA/sisal biocomposites. It was therefore necessary to stablish in-depth analyses to point out reliable degradation indicators and correlate the impact of biodegradation to the structural and morphological state of the PLA/sisal biocomposites.
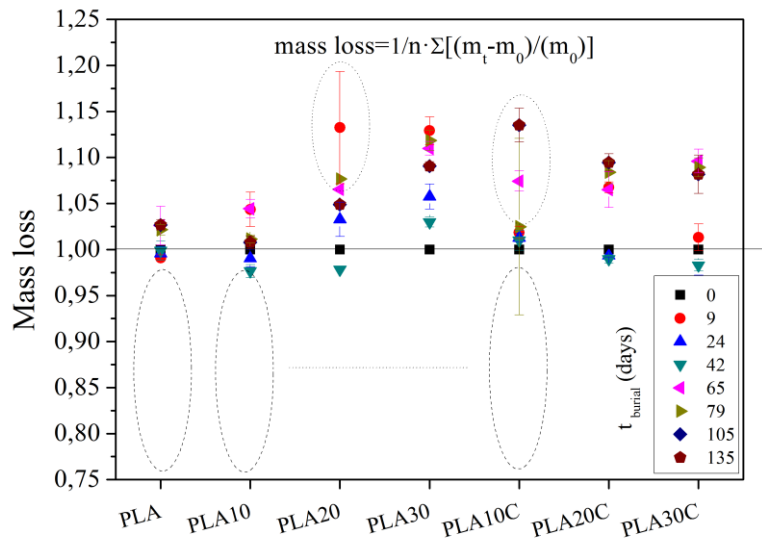
Figure 1. Measurements of mass-loss of PLA/sisal biocomposites according to standard ISO846
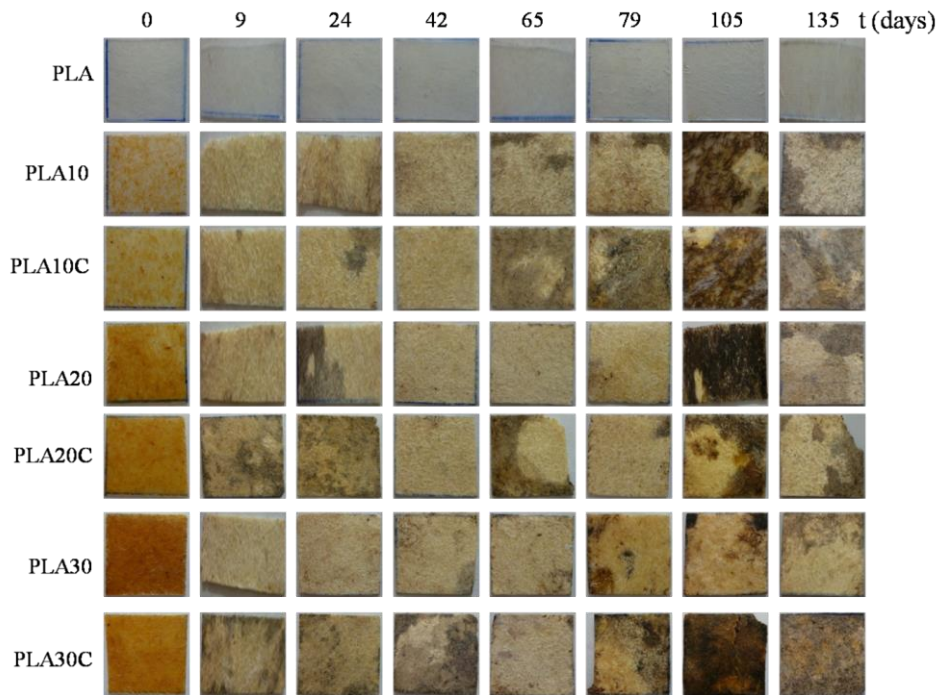

Figure 2. Pictures of PLA/sisal composites subjected to biodegradation in soil

10

3.2. Impact of biodegradation in soil on the chemical structure of PLA/sisal biocomposites

The structural effects of biodegradation in soil on the PLA/sisal biocomposites were assessed in terms of the variation of the molar mass in number M_n, as shown in **Figure 3**.

In comparison to neat PLA, the addition of sisal generally provoked a decrease of M_n of a ~15%, ~24% and ~32% for PLA10, PLA20 and PLA30, respectively. Therefore, the higher the amount of sisal, the higher the hydroxyl groups from fibers can be activated by the thermal treatment during processing, thus leading to more extended hydrolytic chain scission in the PLA/sisal biocomposite. This effect, along with the characteristic intermolecular transesterification during thermo-mechanical treatment [40], is relevant for the reduction of the M_n. This fact is in agreement with the results of *Le Duigou et al* for polylactide/flax biocomposites [43], where the reduction of molar mass was explained as a result of chain breakage in the polymer matrix during processing, which is hindered by the increase of viscosity and shear of the fibre during processing. Similar results were obtained during the preparation of poly(hydroxybutyrate-co-valerate)/sisal biocomposites [9] or polylactide reinforced with cellulose kraft pulp [44].

When the PLA/sisal biocomposites were prepared with coupling agent, additional reductions were registered, giving a total of ~38%, ~45% and ~46% of M_n decrease. The peroxy radical species incorporated by dicumyl peroxide, along with the carboxylic groups present in maleic acid, may have accelerated the chain scission at the temperatures of preparation of composites, leading to a decrease in M_n [45].

Biodegradation in soil affected to the M_n of PLA/sisal biocomposites mainly during the first stages of burial, where the water in the soil can induce hydrolysis [6]. This fact was especially relevant for PLA/sisal biocomposites prepared with coupling agent, which showed most of their M_n reduction after 9 days. Interestingly, the reduction of molar mass during biodegradation in soil seemed slowed down the higher the amount of fibre in the biocomposite was. This fact could be ascribed to the self-development of a protective mechanism against chain scission, as an increase of crystallinity might represent. Actually, the higher the amount of fibre, would mean an increase of nucleation sites for crystallinity, more resistant to scissoring. Therefore, the characterisation of the crystallinity degree was subsequently addressed by means of differential scanning calorimetry.
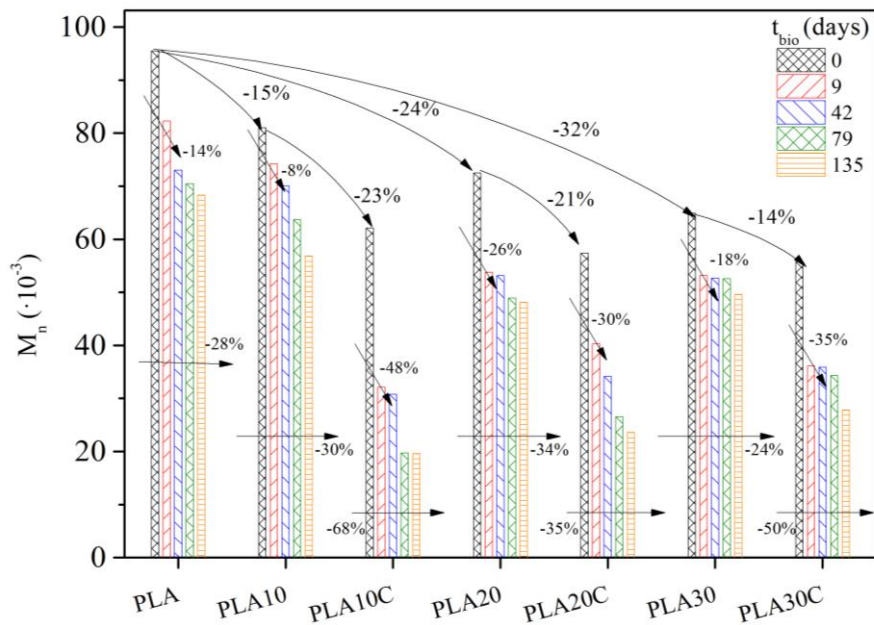
Figure 3. Impact of biodegradation in soil on the molar mass of PLA/sisal biocomposites: influence of fibre amount and use of coupling agent.

3.3. Statistical relevance and interaction of factors of eco-design of PLA/sisal biocomposites on the molar mass in number M_n

In order to evaluate the relative importance of eco-design factors such as the amount of sisal and the use of coupling agent, along with the variable of time of biodegradation in soil, on the molar mass M_n, the statistical factorial analysis (SFA) was applied. In order to validate the reliability of the SFA, the statistical significance of individual and pair-combined factors was checked. P-values below 0.05 and a regression coefficient of 94.64%, positively supported the subsequent interpretation of main-effects plots and interaction-effects plots.

The main-effects plot is shown in **Figure 4**. The grand-mean of samples under study, i.e., the average of M_n of all analyses, plotted as the horizontal line in the graph, was $52.5 \cdot 10^3$ g·mol^{-1}. Only neat PLA, the biocomposites without coupling agent and samples biodegraded up to 9 days showed values above the grand-mean. Therefore, all factors were relevant for the reduction of M_n. In particular, due to the addition of fibre, all biocomposites showed a decrease of M_n, but no significant differences among them was

found. The use of coupling agent was especially relevant in M_n reduction, being as representative as the addition of fibre or even as the action of biodegradation in soil.
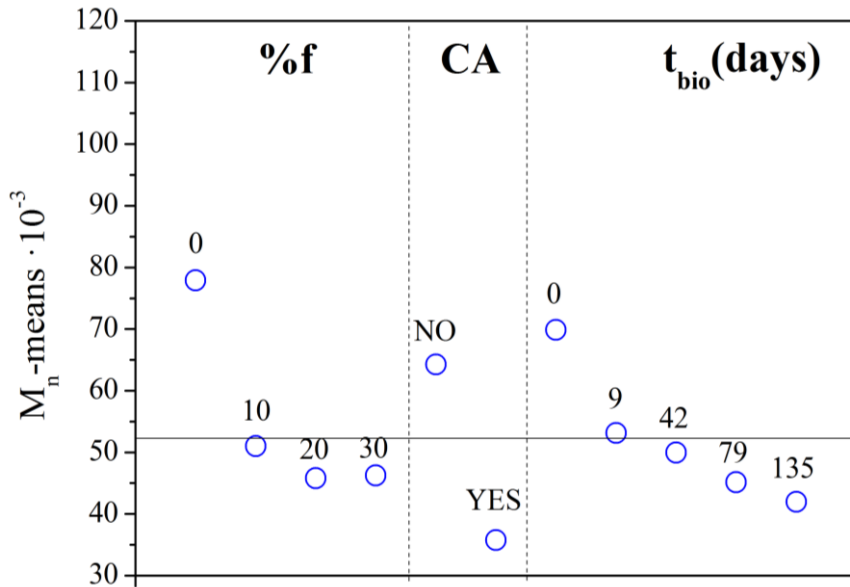

Figure 4. Statistical factorial main-effects plot to assess the impact of biodegradation in soil on the molar mass of PLA/sisal biocomposites: influence of fibre, coupling agent and time of burial.

The interaction-effects plot obtained by the statistical factorial analysis is shown in **Figure 5**.

The interaction between the eco-design factors of addition of sisal and use of coupling agent is shown in **Figure 5a** and **Figure 5d**. The crossing lines showed slight interdependence between both factors. Whereas for biocomposites with no coupling agent, the increase of the amount of fibre was translated into a reduction of the M_n, for biocomposites with coupling agent, the M_n was maintained or even increased with the increment of fibre sin the PLA/sisal biocomposites.

The interaction between the addition of sisal and the time of burial is shown in **Figure 5b** and **Figure 5e.** Both plots showed similar tendencies, which revealed that biodegradation in soil affected the M_n of the PLA/sisal biocomposites regardless the amount of fibre present in their formulation.

Finally, the interaction plots of the use of coupling agent and the time of burial, shown in **Figure 5c** and **Figure 5f**, revealed that biodegradation in soil affected the biocomposites

13

regardless the presence of coupling agent in their formulation, being the main difference encountered between neat PLA and the rest of PLA/sisal biocomposites.
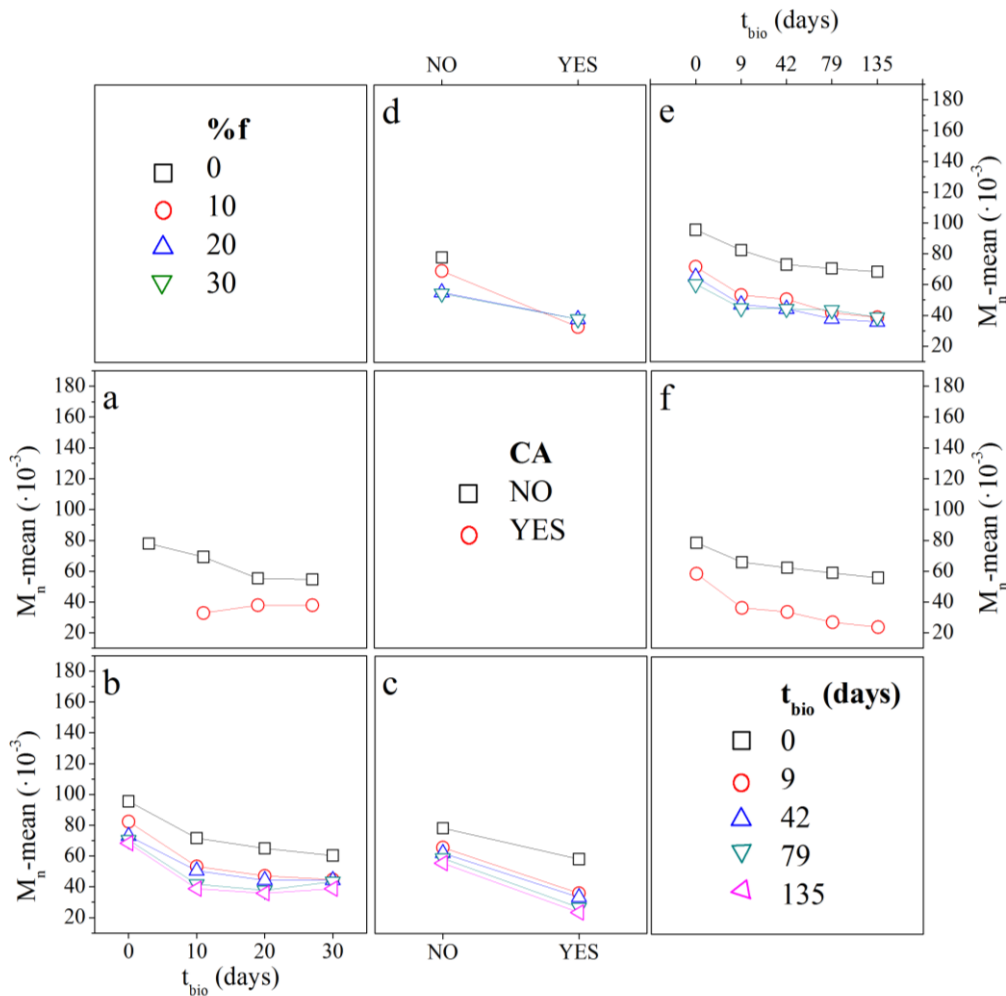

Figure 5. Statistical factorial interaction effects plot of the impact of biodegradation in soil on the molar mass of PLA/sisal biocomposites. Note that legends are shown in the boxes at the diagonal.

3.4. Impact of biodegradation in soil on the morphology and thermal properties

The use of differential scanning calorimetry (DSC) is relevant to deeply understand the effects of any type of degradation [46]–[50]. Particularly for PLA [51]–[53] or PLA/sisal biocomposites [6] several indicators of degradation have been proposed. Accordingly, the thermograms corresponding to the first heating, cooling and second heating obtained by DSC for neat PLA, PLA10, PLA30 and PLA30C subjected to biodegradation in soil are shown in **Figure 6** as model cases to explain the influence of the amount of fibre, the use of coupling agent, along with the effect of biodegradation in soil on the morphology and thermal properties of PLA/sisal biocomposites. The rest of biocomposites lay in between and were omitted for the sake of clarity. During the first and second heating, the following

14

parameters were registered: structural relaxation enthalpy Δh_{SR} and its peak temperature T_{SR}, which is approximated to the glass transition temperature T_G, the cold-crystallisation enthalpy Δh_{CC} and temperature T_{CC} and melting enthalpy Δh_M and temperature T_M. During cooling, the glass transition temperature T_G and the crystallisation enthalpy Δh_C and peak temperature T_C were calculated. All values are shown in

Table 2 for those from the fist heating and the cooling scan and in
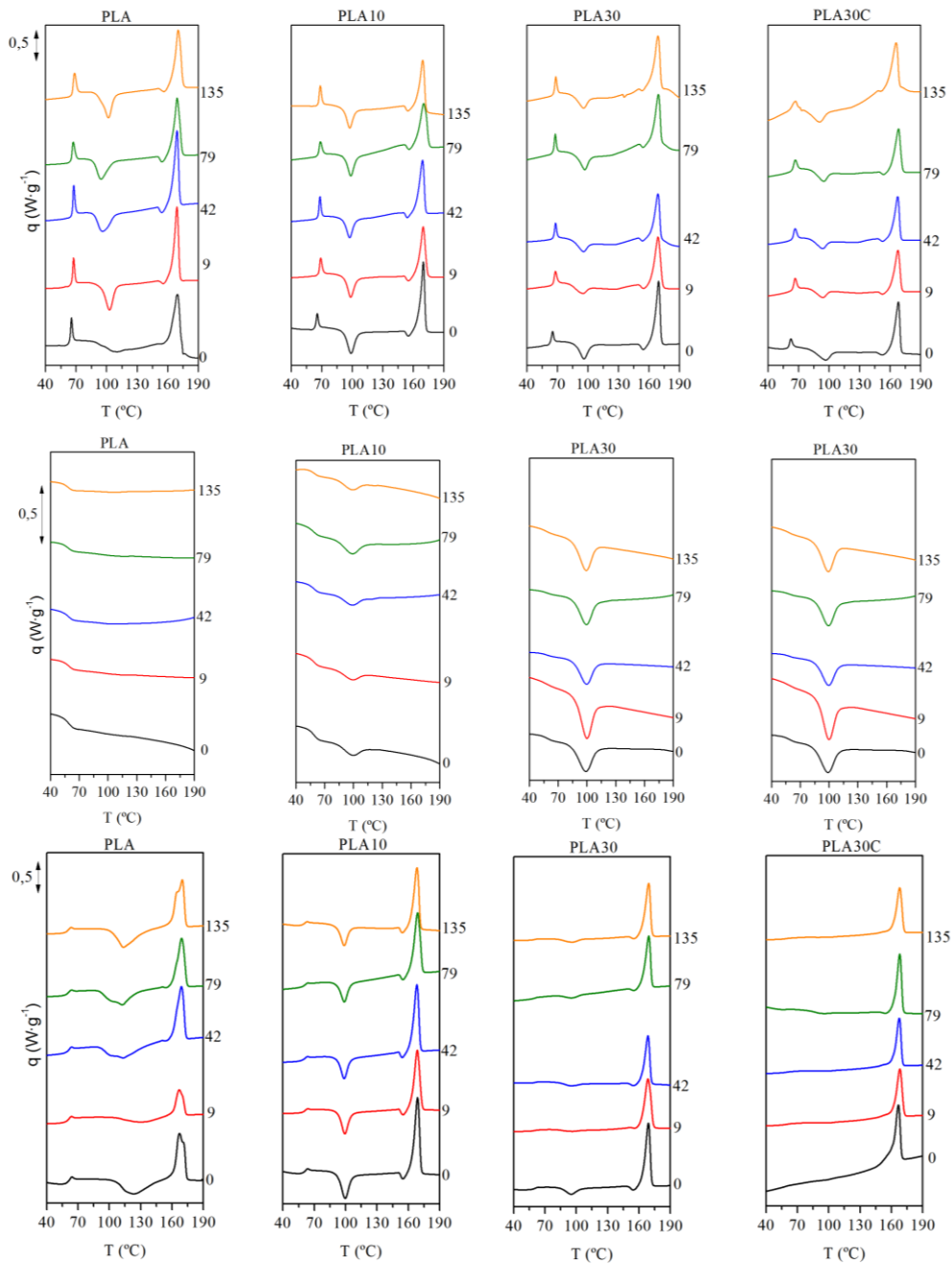
Table 3 for those of the second heating scan.

Figure 6. Calorimetric scans of PLA/sisal biocomposites. From top down, first heating, cooling, second heating. Note that numbers in the right Y-axis represent the days of burial in soil

	t_{bio} (d)	DSC first heating							DSC cooling	
		Δh_{SR} (J·g⁻¹)	T_{SRP} (°C)	Δh_{CC} (J·g⁻¹)	T_{CC} (°C)	Δh_M (J·g⁻¹)	T_M (°C)	T_G (°C)	Δh_C (J/g)	T_C (°C)
PLA	0	6.5 ±0.5	62.7 ±0.1	-33.1 ±3.4	108.7 ±1.3	41.6 ±5.2	173.8 ±0.2	59.2 ±0.5	--- ---	--- ---
	9	6.5 ±0.4	64.4 ±0.1	-33.8 ±1.5	10.29 ±0.1	37.9 ±0.3	172.1 ±0.1	58.4 ±0.1	--- ---	--- ---
	42	6.8 ±1.2	65.1 ±0.3	-37.2 ±0.7	96.3 ±0.2	40.7 ±0.1	171.9 ±0.1	58.5 ±0.1	--- ---	--- ---
	79	6.7 ±0.2	64.5 ±0.1	-32.2 ±0.9	93.3 ±1.7	37.8 ±2.2	174.3 ±0.1	57.7 ±0.1	--- ---	--- ---
	135	6.6 ±0.3	65.2 ±0.2	-34.5 ±0.9	90.3 ±1.2	38.1 ±2.1	172.3 ±0.3	57.8 ±0.2	--- ---	--- ---
PLA10	0	5.6 ±0.7	62.5 ±0.4	-38.8 ±3.1	98.9 ±0.3	41.5 ±1.7	173.1 ±1.1	57.7 ±0.1	-7.1 ±0.2	99.1 ±0.2
	9	6.1 ±0.2	65.8 ±0.2	-33.2 ±2.9	98.1 ±0.3	36.1 ±1.3	173.1 ±0.8	58.3 ±0.6	-6.1 ±0.5	98.6 ±0.1
	42	6.3 ±0.4	65.6 ±0.3	-30.3 ±0.5	97.5 ±0.2	35.9 ±1.5	172.3 ±0.1	57.7 ±0.1	-8.6 ±0.5	98.8 ±0.4
	79	6.6 ±0.2	65.4 ±0.4	-30.7 ±1.8	98.1 ±0.6	43.6 ±0.3	173.7 ±1.9	57.8 ±0.1	-10.1 ±1.2	98.7 ±0.2
	135	6.6 ±0.3	65.3 ±0.1	-31.3 ±0.9	96.3 ±0.3	43.2 ±0.6	173.3 ±1.3	58.1 ±0.4	-6.2 ±0.1	98.6 ±0.1
PLA10C	0	4.7 ±0.2	58.3 ±0.2	-37.6 ±0.2	103.0 ±0.2	39.7 ±0.1	171.4 ±0.2	58.1 ±0.2	-8.1 ±0.3	99.5 ±0.1
	9	6.3 ±0.5	60.3 ±0.6	-36.5 ±0.7	94.4 ±1.5	37.4 ±0.1	169.9 ±0.3	58.3 ±0.7	-19.2 ±1.8	99.6 ±0.2
	42	7.5 ±0.1	60.8 ±0.2	-36.5 ±0.9	95.0 ±0.1	33.9 ±0.3	169.4 ±0.1	58.1 ±0.3	-13.7 ±0.4	99.7 ±0.1
	79	7.2 ±0.3	60.5 ±0.3	-33.3 ±0.3	95.3 ±0.3	35.1 ±0.4	167.6 ±0.3	57.3 ±0.7	-23.5 ±2.2	99.8 ±0.2
	135	7.1 ±0.2	60.6 ±0.3	-34.3 ±0.3	94.3 ±0.3	36.3 ±0.3	167.3 ±0.3	57.7 ±0.8	-26.3 ±1.7	98.5 ±0.1
PLA20	0	3.3 ±0.1	61.3 ±0.2	-36.6 ±2.1	96.7 ±0.1	38.6 ±0.8	172.1 ±0.2	57.0 ±0.9	-15.5 ±1.1	98.8 ±0.1
	9	6.3 ±0.1	65.8 ±0.4	-31.8 ±2.0	97.3 ±0.5	34.7 ±0.6	172.7 ±1.3	56.8 ±1.2	-19.9 ±0.1	98.9 ±0.4
	42	5.3 ±0.4	65.6 ±0.2	-27.6 ±1.6	96.9 ±0.2	35.0 ±2.2	171.7 ±0.7	57.4 ±0.4	-17.3 ±0.6	98.9 ±0.2
	79	5.6 ±0.2	65.4 ±0.3	-28.7 ±1.9	97.4 ±0.5	43.4 ±0.7	173.2 ±1.6	58.1 ±0.8	-21.1 ±3.2	98.9 ±0.2
	135	5.4 ±0.3	65.3 ±0.3	-29.8 ±2.3	96.3 ±0.3	41.2 ±0.6	173.3 ±1.3	58.3 ±0.7	-15.6 ±2.1	98.6 ±0.5
PLA20C	0	3.9 ±0.2	58.4 ±0.3	-33.4 ±2.2	99.2 ±0.3	39.7 ±1.3	171.8 ±0.2	57.0 ±1.1	-18.2 ±0.2	99.6 ±0.6
	9	6.4 ±0.1	62.8 ±1.2	-33.1 ±0.3	95.34 ±1.4	32.3 ±0.7	169.8 ±0.6	57.4 ±1.3	-22.2 ±1.2	101.2 ±0.3
	42	5.3 ±0.8	62.2 ±0.2	-29.6 ±3.1	94.4 ±0.7	36.4 ±3.1	170.6 ±0.4	57.3 ±0.4	-28.7 ±3.1	101.3 ±0.1
	79	5.7 ±0.1	61.8 ±0.3	-30.9 ±1.3	94.5 ±0.1	35.7 ±1.1	169.3 ±1.1	57.4 ±0.5	-28.9 ±0.3	101.9 ±0.1
	135	5.5 ±0.2	62.1 ±0.3	-32.1 ±1.9	93.2 ±0.3	34.3 ±1.8	169.3 ±1.3	56.8 ±0.8	-25.3 ±1.3	100.5 ±0.1
PLA30	0	3.7 ±0.2	62.3 ±0.1	-29.7 ±3.5	96.0 ±0.2	33.3 ±1.3	172.3 ±0.2	57.1 ±0.7	-17.9 ±0.1	98.9 ±0.2
	9	4.1 ±0.7	65.2 ±0.1	-27.6 ±3.4	95.8 ±1.6	36.5 ±0.8	172.6 ±1.3	55.1 ±0.1	-27.6 ±1.9	100.2 ±0.1
	42	5.3 ±0.2	65.0 ±0.4	-25.6 ±3.3	95.6 ±0.1	38.3 ±1.2	172.0 ±0.1	56.8 ±0.4	-17.4 ±2.7	99.6 ±0.5
	79	5.7 ±0.3	64.9 ±0.2	-32.6 ±1.4	96.8 ±0.1	40.6 ±1.4	172.2 ±0.4	57.4 ±0.6	-20.1 ±0.6	99.5 ±0.1
	135	5.2 ±0.4	64.7 ±0.3	-30.3 ±1.3	95.3 ±0.2	39.8 ±1.6	172.3 ±0.3	57.4 ±1.2	-15.6 ±2.1	98.7 ±0.4
PLA30C	0	3.5 ±0.2	59.3 ±0.2	-24.9 ±0.2	96.6 ±0.1	33.5 ±1.6	170.9 ±0.2	55.3 ±0.1	-24.3 ±1.0	101.1 ±0.2
	9	4.3 ±0.5	63.5 ±0.1	-24.7 ±0.3	93.7 ±0.1	29.1 ±0.4	171.4 ±0.1	56.3 ±0.5	-24.9 ±0.9	101.9 ±0.2
	42	4.5 ±0.3	63.4 ±0.4	-28.2 ±3.1	93.5 ±0.1	29.9 ±2.1	170.4 ±0.1	54.6 ±0.6	-24.5 ±3.6	102.5 ±0.2
	79	4.5 ±0.4	62.6 ±1.2	-27.8 ±1.3	92.1 ±0.3	31.4 ±0.1	171.2 ±1.2	56.3 ±0.7	-24.9 ±2.6	102.4 ±0.1
	135	4.6 ±0.6	63.5 ±0.3	-30.3 ±1.9	91.3 ±0.3	31.2 ±1.2	171.3 ±1.3	57.3 ±0.8	-32.8 ±2.2	103.2 ±0.5

Table 2. Calorimetric results from the first heating scan and cooling scan of PLA and PLA/sisal biocomposites

DSC second heating

	t_{bio} (d)	Δh_{SR} (J·g^{-1})	$T_{SR/G}$ (ºC)	Δh_{CC} (J·g^{-1})	T_{CC} (ºC)	Δh_{M} (J·g^{-1})	T_{m} (ºC)
PLA	0	1.9 ±0.3	60.4 ±0.1	-35.3 ±1.3	122.2 ±0.1	36.8 ±3.1	173.6 ±0.5
	9	1.5 ±0.3	60.2 ±0.2	-35.4 ±1.2	123.1 ±1.6	36.2 ±2.3	173.3 ±0.1
	42	1.6 ±0.6	60.4 ±0.2	-37.3 ±1.3	113.3 ±0.1	38.9 ±3.1	172.7 ±0.4
	79	1.1 ±0.3	60.2 ±0.1	-33.3 ±1.4	113.3 ±1.8	35.2 ±2.3	173.9 ±0.3
	135	0.5 ±0.1	59.9 ±0.4	-36.7 ±2.1	113.6 ±0.2	37.2 ±3.4	173.1 ±0.1
PLA10	0	1.4 ±0.5	60.2 ±0.1	-32.8 ±1.3	99.6 ±0.1	41.5 ±1.6	172.3 ±0.2
	9	1.3 ±0.3	60.3 ±0.1	-28.4 ±1.2	992 ±0.1	35.9 ±1.2	172.4 ±0.9
	42	1.5 ±0.3	60.4 ±0.3	-28.7 ±3.1	98.7 ±0.1	39.2 ±3.1	171.5 ±0.1
	79	0.2 ±0.1	60.1 ±0.1	-29.4 ±2.1	98.3 ±0.1	34.7 ±2.4	172.5 ±1.5
	135	0.4 ±0.2	59.5 ±0.1	-23.9 ±1.2	98.2 ±0.2	34.3 ±1.2	171.5 ±0.1
PLA10C	0	--- ---	59.7 ±0.1	-34.9 ±1.3	102.2 ±0.3	40.7 ±2.5	171.2 ±0.1
	9	--- ---	58.5 ±0.6	-19.83 ±1.4	100.4 ±0.3	36.2 ±3.1	170.3 ±0.4
	42	--- ---	57.5 ±0.1	-13.37 ±2.1	98.6 ±0.7	33.1 ±1.8	169.4 ±0.4
	79	--- ---	56.4 ±0.6	-10.82 ±2.3	96.2 ±0.1	36.8 ±1.7	168.1 ±0.2
	135	--- ---	56.3 ±0.5	-6.05 ±1.8	96.7 ±0.3	37.6 ±2.4	169.2 ±0.3
PLA20	0	--- ---	60.1 ±0.3	-22.3 ±1.7	94.9 ±0.3	37.7 ±1.9	171.9 ±0.1
	9	--- ---	59.7 ±0.7	-21.6 ±1.4	95.9 ±0.1	35.5 ±1.8	172.2 ±1.3
	42	--- ---	60.3 ±0.7	-18.7 ±2.1	96.5 ±0.3	34.7 ±3.2	171.4 ±0.2
	79	--- ---	59.9 ±1.0	-14.7 ±1.9	96.8 ±0.2	39.14 ±2.3	172.3 ±1.1
	135	--- ---	59.8 ±0.9	-16.7 ±1.2	96.2 ±0.1	39.32 ±2.4	171.2 ±0.5
PLA20C	0	--- ---	59.7 ±0.1	-19.9 ±1.3	94.9 ±0.1	37.9 ±1.6	170.9 ±0.1
	9	--- ---	59.6 ±0.6	-7.8 ±0.7	95.9 ±1.3	31.4 ±2.4	170.3 ±0.2
	42	--- ---	59.0 ±0.7	-7.7 ±0.7	96.5 ±0.1	35.9 ±1.5	170.5 ±0.6
	79	--- ---	61.4 ±1.2	-3.2 ±1.5	96.8 ±0.1	36.4 ±2.8	169.1 ±0.7
	135	--- ---	56.6 ±0.2	-3.0 ±0.8	96.2 ±0.2	36.5 ±1.9	169.6 ±1.5
PLA30	0	--- ---	60.8 ±0.3	-12.3 ±1.3	99.1 ±0.3	33.2 ±1.7	171.9 ±0.1
	9	--- ---	60.8 ±0.2	-9.6 ±1.5	97.0 ±0.4	31.2 ±2.3	172.6 ±1.3
	42	--- ---	60.2 ±0.2	-8.4 ±1.1	97.2 ±0.1	29.4 ±2.4	171.6 ±0.1
	79	--- ---	59.1 ±0.2	-8.5 ±0.7	97.2 ±0.3	29.4 ±1.8	172.0 ±0.4
	135	--- ---	61.1 ±1.2	-8.7 ±0.4	97.5 ±1.1	31.2 ±1.6	173.0 ±1.1
PLA30C	0	--- ---	59.7 0.1	-10.4 ±0.7	94.5 ±0.1	31.2 ±2.4	171.0 ±0.1
	9	--- ---	59.2 1.9	-1.2 ±1.2	94.3 ±0.2	314 ±2.1	171.7 ±0.2
	42	--- ---	62.5 1.3	-0.5 ±1.3	95.3 ±0.3	30.1 ±1.8	170.5 ±0.1
	79	--- ---	60.5 1.3	--- ---	94.3 ±0.2	36.8 ±2.1	17.2 ±1.2
	135	--- ---	60.9 0.3	--- ---	94.7 ±0.2	43.5 ±1.3	169.6 ±0.2

Table 3. Calorimetric results from the second heating scan of PLA and PLA/sisal biocomposites

Biodegradation in soil provoked scission of the PLA matrix, as suggested by SEC results. During the first scan, the parameter that showed the most remarkable tendency was the cold-crystallisation temperature T_{CC}, which decreased with the time of burial in soil, being more relevant with those PLA/sisal biocomposites prepared with coupling agent. Therefore, T_{CC}, was an appropriate indicator of chain scission, which pointed out the liability of shorter macromolecular segments to rearrange into a crystalline morphology [28].

The impact on the amorphous fraction could be obtained from the glass transition temperature T_G of the cooling scan. According to the Fox-Flory relationship between the molar mass M_n and the glass transition temperature T_G [54], although the chain scission reduced the molar mass of the neat PLA, it was still high enough to keep the T_G in the invariant regime, which was in agreement with the absence of disintegration of samples.

At the second heating scan, a clear reduction of the cold-crystallisation enthalpy and a maintenance or slight increase of the melting enthalpy were encountered as a function of time of burial in soil, being more representative for those PLA/sisal biocomposites prepared with coupling agent.

Biodegradation in soil had a clear impact on the crystallinity of PLA/sisal biocomposites. In order to quantify the degree of influence of the eco-design factors under study, i.e, amount of fibre and use of coupling agent, along with the variable of time of burial in soil, the degree of crystallinity was calculated as X_C (%)$=(1-m_f)^{-1} \cdot [(\Delta h_M - |\Delta h_{CC}|] \cdot \Delta h_{M0}^{-1} \cdot 100$, where m_f represents the weight fraction of sisal in the PLA/sisal biocomposite and Δh_{M0} is the melting enthalpy of a 100% crystalline PLA [55]. The evolution of X_C is given in **Figure 7** for all biocomposites subjected to biodegradation in soil. Neat PLA showed very low X_C, due to its amorphous character, in agreement with previous studies [6], [7]. The addition of fibre almost three-folded X_C for PLA10, six-folded for PLA20 and nine-folded for PLA30, with no apparent relevance of the coupling agent during the preparation of the biocomposites, prior to biodegradation in soil. This was in agreement with the reported formation of transcrystalline regions between fibre and polymers such as polypropylene/sisal [56], polypropylene/flax , polylactide/hemp [57] or thermoplastic starch/cellulose [58], among others, related to the presence of nucleation sites in the fibre where the matrix can develop a crystalline fraction along the longitudinal axis of fibres.

The use of coupling agent was not relevant for the modification of the initial X_C. Only in the case of PLA10C, this biocomposite showed lower X_C due to the restriction of available molecules in uncoupled biocomposites which slowed down the crystallisation effect of fibres, as reported for polypropylene/kenaf composites [59]. The rest of biocomposites showed no specific variation of initial X_C, as also reported for composites such as polypropylene/palm [60].

The difference of coupled and uncoupled biocomposites was relevant in terms of performance during burial. In agreement with the evolution of molar mass due to biodegradation in soil, the first stages of burial were the most relevant. In particular, after 9 days of exposure in soil, the PLA/sisal composites with coupling agent developed almost half of the total X_C increase. During the whole biodegradation process, the PLA/sisal biocomposites without coupling agent just showed small variations of X_C. In contrasts, the evolution registered for PLA/sisal biocomposites with coupling agent was more significant.
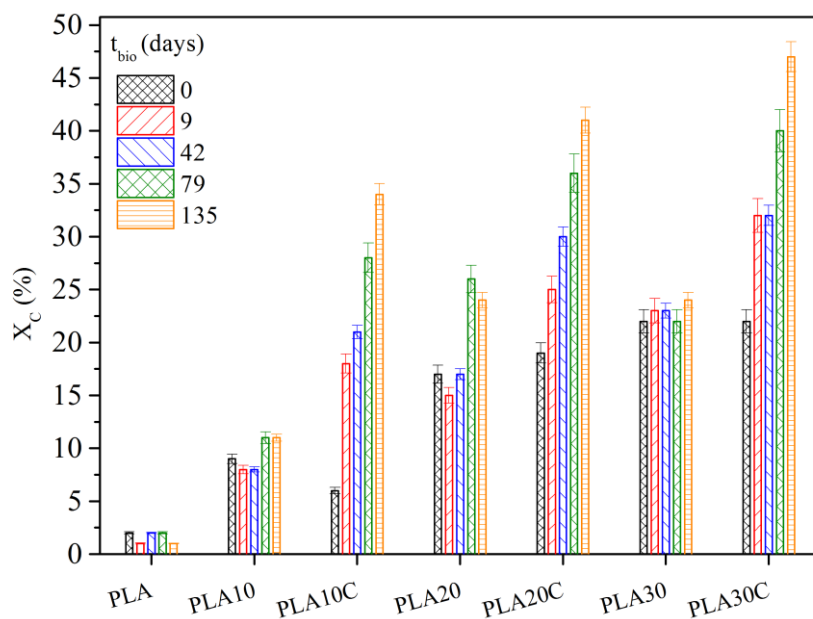

Figure 7. Impact of biodegradation in soil on the degree of crystallinity of the PLA/sisal biocomposites: influence of fibre amount and use of coupling agent.

3.5. Statistical relevance and interaction of factors of eco-design of PLA/sisal biocomposites on the crystallinity degree X_C

In order to evaluate the relative importance of eco-design factors such as the amount of sisal and the use of coupling agent, along with the variable of time of biodegradation in soil, on the crystallinity degree X_C, the statistical factorial analysis (SFA) was applied. In order to validate the meaningfulness of the SFA, the statistical significance of individual and pair-combined factors was evaluated. Low p-values < 0.05 and high regression coefficient of 99.06%, certainly supported the subsequent explanation of the main-effects plots and interaction-effects plots.

The main-effects plots, obtained by the statistical factorial analysis, are shown in **Figure 8**. The grand-mean of samples under study was 20%. As previously suggested, both eco-design factors were relevant for the development of X_C: first, the addition of fibre, which gave and increment of X_C means from ~ 2 % to ~ 30 % from neat PLA to PLA/sisal biocomposites with 30 wt% of sisal, with and without coupling agent; second, the use of coupling agent, which gave and increment of X_C means from ~ 15 % to ~ 30 % from PLA/sisal composites without coupling agent to those with coupling agent. Finally, biodegradation in soil gave and increment of X_C means from ~ 15 % to ~ 27 % from 0 to 135 days of burial, in the same level of influence as the use of coupling agent.
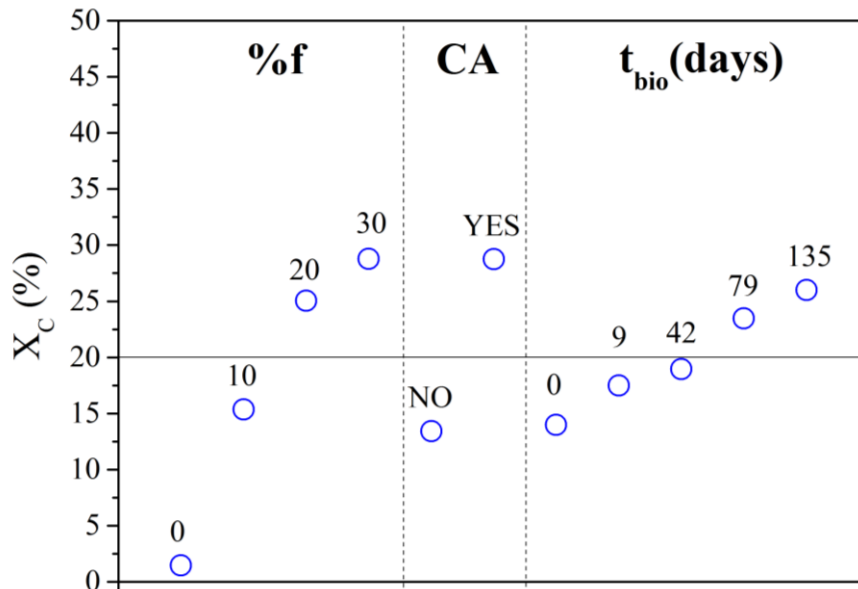

Figure 8. Statistical factorial main-effects plot to assess the impact of biodegradation in soil on the crystallinity degree of PLA/sisal biocomposites: influence of fibre, coupling agent and time of burial

The interaction-effects plot obtained by the statistical factorial analysis is shown in **Figure 9**. The interaction between the eco-design factors of addition of sisal and use of coupling agent is shown in **Figure 9a** and **Figure 9d**. In contrast to what was shown by the molar mass M_n, there was no particular interaction between both factors, as suggested by the parallel lines.

The interaction between the addition of sisal and the time of burial is shown in **Figure 9b** and **Figure 9e.** They showed significant dependence for the evolution of X_C from neat PLA to PLA/sisal biocomposites during biodegradation in soil, with slight variations among PLA/sisal biocomposites.

Finally, the interaction plots of the use of coupling agent and the time of burial, shown in **Figure 9c** and **Figure 9f**. They clearly stated that PLA/sisal biocomposites with coupling agent were more sensitive to the evolution of X_C, in contrast to PLA/sisal biocomposites without coupling agent, which were almost insensitive to biodegradation in soil.
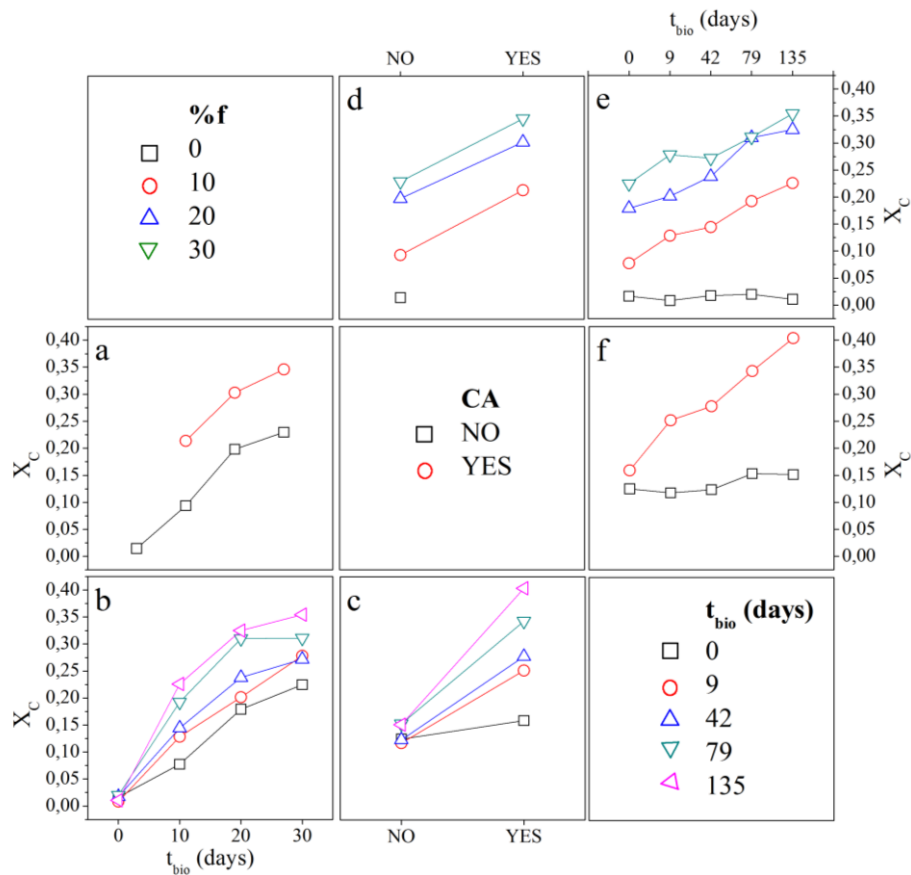

Figure 9. Statistical factorial interaction effects plot of the impact of biodegradation in soil on the degree of crystallinity of PLA/sisal biocomposites. Note that legends are shown in the boxes at the diagonal.

3.6. Outline of results

The influence of the addition of fibre and the presence of coupling agent in the PLA/sisal biocomposites on their behaviour throughout biodegradation in soil can be summarised hereby in terms of molar mass M_n and crystallinity degree X_C.

Due to the addition of fibre, without presence of coupling agent:

(i) A reduction of M_n caused by chain scission due to thermo-mechanical degradation during the preparation of the biocomposites was found.

(ii) An increase of X_C promoted by the rearrangement of polymer segments of the PLA matrix at nucleation sites of the sisal fibres was encountered.

(iii) Biodegradation in soil reduced the M_n mainly during the first days of burial, with independence of the amount of fibre present in the biocomposite. There was no relevant increment of X_C associated to the molar mass reduction.

Due to the presence of coupling agent in the PLA/sisal biocomposites:

(i) The reduction of M_n during the preparation of the biocomposites was enhanced, due to the action of the peroxide groups present in the coupling agent.

(ii) The increase of X_C was slightly affected during the preparation of biocomposites,

(iii) During biodegradation in soil, the chain scission process was intensified, which affected both the reduction of M_n and the related increase of X_C.

The correlation between molar mass and crystallinity degree during biodegradation in soil is finally pictured in **Figure 10** to support the discussions given by statistical factorial analysis. Biodegradation in soil mainly affected PLA/sisal biocomposites prepared with coupling agent, which gave out massive chain scission, and thus remarkably reduced molar mass and promoted crystalline fraction. These results may help interpret the competitive balance between degradation and assimilation, since degradation not only causes chain scission, which would release short polymer segments, easily transformable by microorganisms, but also provokes crystallisation, which might difficult their catabolism.
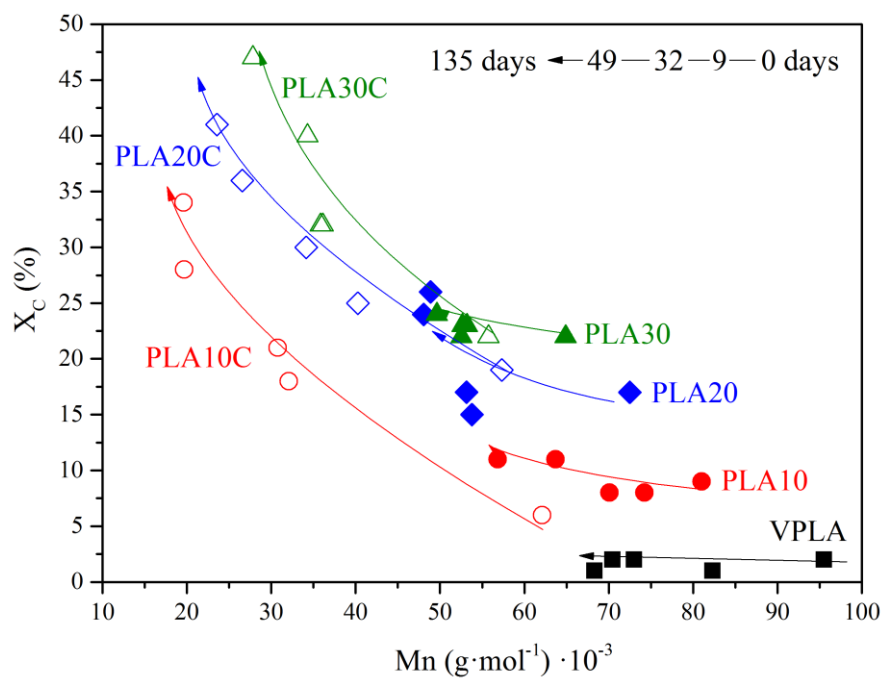
Figure 10. Correlation between degree of crystallinity and molar mass along biodegradation in soil

4. Conclusions

The eco-design of biocomposites should take into account the end-of-life scenario. The addition of sisal fibre and the use of coupling agent in PLA/sisal biocomposites will play a role in the balance between the facilitation of microbial assimilation of polymer segments due to chain scission of the polymer matrix, or its hindrance by the promotion of crystalline fractions.

The addition of fibre was more relevant in terms of crystallinity degree -which increased according to the amount of sisal, due to the augment of nucleation sites-, than in terms of molar mass – which was quite similar between biocomposites and just remarkably different in comparison to neat PLA. During biodegradation in soil, hydrolytic chain scission provoked a reduction of molar mass, and a slight increment of crystallinity degree.

The coupling agent was the most relevant factor in the design of PLA/sisal biocomposites, since the presence of peroxide groups accelerated chain scission and subsequent crystalline nucleation, both after the preparation of the PLA/sisal biocomposites and mainly during biodegradation in soil.

References

[1]   M. J. John and S. Thomas, "Biofibres and biocomposites," *Carbohydr. Polym.*, vol. 71, no. 3, pp. 343–364, 2008.

[2]   H. P. S. A. Khalil, A. M. Issam, M. T. A. Shakri, R. Suriani, and A. Y. Awang, "Conventional agro-composites from chemically modified fibres," *Ind. Crops Prod.*, vol. 26, no. 3, pp. 315–323, 2007.

[3]   F. P. La Mantia and M. Morreale, "Green composites: A brief review," *Compos. Part A Appl. Sci. Manuf.*, vol. 42, no. 6, pp. 579–588, 2011.

[4]   M. Braungart, W. McDonough, and A. Bollinger, "Cradle-to-cradle design: creating healthy emissions – a strategy for eco-effective product and system design," *J. Clean. Prod.*, vol. 15, no. 13–14, pp. 1337–1348, Sep. 2007.

[5]   C. R. Álvarez-Chávez, S. Edwards, R. Moure-Eraso, and K. Geiser, "Sustainability of bio-based plastics: general comparative analysis and recommendations for improvement," *J. Clean. Prod.*, vol. 23, no. 1, pp. 47–56, Mar. 2012.

[6]   O. Gil-Castell, J. Badia, T. Kittikorn, E. Strömberg, A. Martínez-Felipe, M. Ek, S. Karlsson, and A. Ribes-Greus, "Hydrothermal ageing of polylactide/sisal biocomposites. Studies of water absorption behaviour and physicochemical performance," *Polym. Degrad. Stab.*, vol. 132, pp. 87–96, 2016.

[7]   O. Gil-Castell, J. D. Badia, T. Kittikorn, E. Strömberg, M. Ek, S. Karlsson, and A. Ribes-Greus, "Impact of hydrothermal ageing on the thermal stability, morphology and viscoelastic performance of PLA/sisal biocomposites," *Polym. Degrad. Stab.*, 2016.

[8]   Y. Wang, B. Tong, S. Hou, M. Li, and C. Shen, "Transcrystallization behavior at the poly (lactic acid)/sisal fibre biocomposite interface," *Compos. Part A Appl. Sci. Manuf.*, vol. 42, no. 1, pp. 66–74, 2011.

[9]   J. D. Badia, T. Kittikorn, E. Strömberg, L. Santonja-Blasco, A. Martínez-Felipe, A. Ribes-Greus, M. Ek, and S. Karlsson, "Water absorption and hydrothermal performance of PHBV/sisal biocomposites," *Polym. Degrad. Stab.*, vol. 108, pp. 166–174, Oct. 2014.

[10]   R. Dangtungee, J. Tengsuthiwat, P. Boonyasopon, and S. Siengchin, "Sisal natural

fiber/clay-reinforced poly (hydroxybutyrate-co-hydroxyvalerate) hybrid composites," *J. Thermoplast. Compos. Mater.*, vol. 28, no. 6, pp. 879–895, 2015.

[11] V. A. A. Alvarez and A. Vázquez, "Thermal degradation of cellulose derivatives/starch blends and sisal fibre biocomposites," *Polym. Degrad. Stab.*, vol. 84, no. 1, pp. 13–21, Apr. 2004.

[12] V. A. A. Alvarez, R. A. A. Ruseckaite, A. Vázquez, and A. Vazquez, "Degradation of sisal fibre/Mater Bi-Y biocomposites buried in soil," *Polym. Degrad. Stab.*, vol. 91, no. 12, pp. 3156–3162, 2006.

[13] C. R. di Franco, V. P. Cyras, J. P. Busalmen, R. A. Ruseckaite, and A. Vázquez, "Degradation of polycaprolactone/starch blends and composites with sisal fibre," *Polym. Degrad. Stab.*, vol. 86, no. 1, pp. 95–103, 2004.

[14] E. V. R. Almeida, E. Frollini, A. Castellan, and V. Coma, "Chitosan, sisal cellulose, and biocomposite chitosan/sisal cellulose films prepared from thiourea/NaOH aqueous solution," *Carbohydr. Polym.*, vol. 80, no. 3, pp. 655–664, 2010.

[15] S. Mishra, A. K. Mohanty, L. T. Drzal, M. Misra, and G. Hinrichsen, "A review on pineapple leaf fibers, sisal fibers and their biocomposites," *Macromol. Mater. Eng.*, vol. 289, no. 11, pp. 955–974, 2004.

[16] T. Lu, S. Liu, M. Jiang, X. Xu, Y. Wang, Z. Wang, J. Gou, D. Hui, and Z. Zhou, "Effects of modifications of bamboo cellulose fibers on the improved mechanical properties of cellulose reinforced poly(lactic acid) composites," *Compos. Part B Eng.*, vol. 62, pp. 191–197, 2014.

[17] T. Kittikorn, E. Strömberg, M. Ek, and S. Karlsson, "The effect of surface modifications on the mechanical and thermal properties of empty fruit bunch oil palm fibre PP biocomposites," *Polym. from Renew. Resour.*, vol. 3, no. 3, pp. 79–100, 2012.

[18] A. Espert, W. Camacho, and S. Karlson, "Thermal and thermomechanical properties of biocomposites made from modified recycled cellulose and recycled polypropylene," *J. Appl. Polym. Sci.*, vol. 89, no. 9, pp. 2353–2360, Aug. 2003.

[19] Y. Xie, C. A. S. Hill, Z. Xiao, H. Militz, and C. Mai, "Silane coupling agents used

for natural fiber/polymer composites: A review," *Compos. Part A Appl. Sci. Manuf.*, vol. 41, no. 7, pp. 806–819, 2010.

[20]   H. Nakatani, K. Hashimoto, K. Miyazaki, and M. Terano, "Cellulose/syndiotactic polypropylene composites: effects of maleated polypropylene as a compatibilizer and silanized cellulose on the morphology and tensile properties," *J. Appl. Polym. Sci.*, vol. 113, no. 3, pp. 2022–2029, 2009.

[21]   L. Petersson, K. Oksman, and A. P. Mathew, "Using maleic anhydride grafted poly (lactic acid) as a compatibilizer in poly (lactic acid)/layered-silicate nanocomposites," *J. Appl. Polym. Sci.*, vol. 102, no. 2, pp. 1852–1862, 2006.

[22]   K. Issaadi, A. Habi, Y. Grohens, and I. Pillin, "Maleic anhydride-grafted poly (lactic acid) as a compatibilizer in poly (lactic acid)/graphene oxide nanocomposites," *Polym. Bull.*, vol. 73, no. 7, pp. 2057–2071, 2016.

[23]   D. K. A. Barnes, F. Galgani, R. C. Thompson, and M. Barlaz, "Accumulation and fragmentation of plastic debris in global environments," *Philos. Trans. R. Soc. B Biol. Sci.*, vol. 364, no. 1526, p. 1985 LP-1998, Jun. 2009.

[24]   J. D. Badia, O. Gil-Castell, and A. Ribes-Greus, "Long-term properties and end-of-life of polymers from renewable resources," *Polym. Degrad. Stab.*, 2017.

[25]   M. Bhattacharya, R. L. Reis, V. Correlo, L. Boesel, K. Dean, L. Yu, S. Matsumura, and G. Madras, *Biodegradable Polymers for Industrial Applications*. Elsevier, 2005.

[26]   A. A. Shah, F. Hasan, A. Hameed, and S. Ahmed, "Biological degradation of plastics: a comprehensive review.," *Biotechnol. Adv.*, vol. 26, no. 3, pp. 246–65, Jan. 2008.

[27]   E. N. ISO, "846. 1997," *Plast. action Microorg.*, 1997.

[28]   J. D. Badía, L. Santonja-Blasco, R. Moriana, and A. Ribes-Greus, "Thermal analysis applied to the characterization of degradation in soil of polylactide: II. on the thermal stability and thermal decomposition kinetics," *Polym. Degrad. Stab.*, vol. 95, no. 11, pp. 2192–2199, 2010.

[29]   L. Santonja-Blasco, R. Moriana, J. D. D. Badía, and A. Ribes-Greus, "Thermal analysis applied to the characterization of degradation in soil of polylactide: I.

Calorimetric and viscoelastic analyses," *Polym. Degrad. Stab.*, vol. 95, no. 11, pp. 2192–2199, 2010.

[30] L. Santonja-Blasco, a. Ribes-Greus, and R. G. Alamo, "Comparative thermal, biological and photodegradation kinetics of polylactide and effect on crystallization rates," *Polym. Degrad. Stab.*, vol. 98, no. 3, pp. 771–784, Mar. 2013.

[31] M. J. Kay, R. W. McCabe, and L. H. G. Morton, "Chemical and physical changes occurring in polyester polyurethane during biodegradation," *Int. Biodeterior. Biodegradation*, vol. 31, no. 3, pp. 209–225, 1993.

[32] S. Atarijabarzadeh, E. Strömberg, and S. Karlsson, "Inhibition of biofilm formation on silicone rubber samples using various antimicrobial agents," *Int. Biodeterior. Biodegrad.*, vol. 65, no. 8, pp. 1111–1118, 2011.

[33] K. Bajer, A. Richert, D. Bajer, and J. Korol, "Biodegradation of plastified starch obtained by corotation twin-screw extrusion," *Polym. Eng. Sci.*, vol. 52, no. 12, pp. 2537–2542, Dec. 2012.

[34] M. Karamanlioglu, R. Preziosi, and G. D. Robson, "Abiotic and biotic environmental degradation of the bioplastic polymer poly(lactic acid): A review," *Polym. Degrad. Stab.*, vol. 137, pp. 122–130, 2017.

[35] E. F. Gómez and F. C. Michel, "Biodegradability of conventional and bio-based plastics and natural fiber composites during composting, anaerobic digestion and long-term soil incubation," *Polym. Degrad. Stab.*, vol. 98, no. 12, pp. 2583–2591, Dec. 2013.

[36] G. E. P. Box, "HUNTER, j. S.; HUNTER, WG Statistics for experiments: designs, innovation and discovery." New Jersey: John Wiley & Sons, Inc, 2005.

[37] T. Kittikorn, "Tuning the long-term properties to control biodegradation by surface modifications of agricultural fibres in biocomposites." KTH Royal Institute of Technology, 2013.

[38] I. S. O. Standard, "Plastics—standards atmospheres for conditioning and testing," *Ref. EN ISO*, vol. 291, 1997.

[39] J. D. Badía, E. Strömberg, A. Ribes-Greus, and S. Karlsson, "A statistical design

of experiments for optimizing the MALDI-TOF-MS sample preparation of polymers. An application in the assessment of the thermo-mechanical degradation mechanisms of poly (ethylene terephthalate)," *Anal. Chim. Acta*, vol. 692, no. 1–2, pp. 85–95, 2011.

[40]   J. D. Badía, E. Strömberg, A. Ribes-Greus, and S. Karlsson, "Assessing the MALDI-TOF MS sample preparation procedure to analyze the influence of thermo-oxidative ageing and thermo-mechanical degradation on poly (Lactide)," *Eur. Polym. J.*, vol. 47, no. 7, pp. 1416–1428, 2011.

[41]   A. Espert, F. Vilaplana, and S. Karlsson, "Comparison of water absorption in natural cellulosic fibres from wood and one-year crops in polypropylene composites and its influence on their mechanical properties," *Compos. Part A Appl. Sci. Manuf.*, vol. 35, no. 11, pp. 1267–1276, 2004.

[42]   Y. Li, Y. W. Mai, and L. Ye, "Sisal fibre and its composites: a review of recent developments," *Compos. Sci. Technol.*, vol. 60, no. 11, pp. 2037–2055, 2000.

[43]   A. Le Duigou, P. Davies, and C. Baley, "Seawater ageing of flax/poly(lactic acid) biocomposites," *Polym. Degrad. Stab.*, vol. 94, no. 7, pp. 1151–1162, 2009.

[44]   S. Virtanen, L. Wikström, K. Immonen, U. Anttila, and E. Retulainen, "Cellulose kraft pulp reinforced polylactic acid (PLA) composites : effect of fibre moisture content," vol. 3, no. May, pp. 756–769, 2016.

[45]   S. W. Hwang, S. B. Lee, C. K. Lee, J. Y. Lee, J. K. Shim, S. E. M. Selke, H. Soto-Valdez, L. Matuana, M. Rubino, and R. Auras, "Grafting of maleic anhydride on poly(L-lactic acid). Effects on physical and mechanical properties," *Polym. Test.*, vol. 31, no. 2, pp. 333–344, 2012.

[46]   F. Vilaplana and S. Karlsson, "Quality concepts for the improved use of recycled polymeric materials: A review," *Macromol. Mater. Eng.*, vol. 293, no. 4, pp. 274–297, 2008.

[47]   J. D. Badía, F. Vilaplana, S. Karlsson, and A. Ribes-Greus, "Thermal analysis as a quality tool for assessing the influence of thermo-mechanical degradation on recycled poly(ethylene terephthalate)," *Polym. Test.*, vol. 28, no. 2, pp. 169–175, 2009.

[48] J. D. Badia, E. Strömberg, S. Karlsson, and A. Ribes-Greus, "The role of crystalline, mobile amorphous and rigid amorphous fractions in the performance of recycled poly (ethylene terephthalate) (PET)," *Polym. Degrad. Stab.*, vol. 97, no. 1, pp. 98–107, 2012.

[49] O. Gil-Castell, J. D. Badia, R. Teruel-Juanes, I. Rodriguez, F. Meseguer, and A. Ribes-Greus, "Novel silicon microparticles to improve sunlight stability of raw polypropylene," *Eur. Polym. J.*, vol. 70, pp. 247–261, 2015.

[50] O. Gil-Castell, J. D. Badia, E. Strömberg, S. Karlsson, and A. Ribes-Greus, "Effect of the dissolution time into an acid hydrolytic solvent to taylor electrospun nanofibrous polycaprolactone scaffolds," *Eur. Polym. J.*, vol. 87, pp. 174–187, 2017.

[51] J. D. Badia, E. Strömberg, S. Karlsson, and A. Ribes-Greus, "Material valorisation of amorphous polylactide. Influence of thermo-mechanical degradation on the morphology, segmental dynamics, thermal and mechanical performance," *Polym. Degrad. Stab.*, vol. 97, no. 4, pp. 670–678, 2012.

[52] J. D. Badia and A. Ribes-Greus, "Mechanical recycling of polylactide, upgrading trends and combination of valorization techniques," *Eur. Polym. J.*, vol. 84, pp. 22–39, 2016.

[53] J. D. Badia, L. Santonja-Blasco, A. Martínez-Felipe, and A. Ribes-Greus, "Hygrothermal ageing of reprocessed polylactide," *Polym. Degrad. Stab.*, vol. 97, no. 10, pp. 1881–1890, 2012.

[54] T. G. Fox and P. J. Flory, "The glass temperature and related properties of polystyrene. Influence of molecular weight," *J. Polym. Sci.*, vol. 14, no. 75, pp. 315–319, 1954.

[55] E. W. Fischer, H. J. Sterzel, and G. Wegner, "Investigation of the structure of solution grown crystals of lactide copolymers by means of chemical reactions," in *Aktuelle Probleme der Polymer-Physik IV: Vortr{ä}ge der Arbeitstagung des Fachausschusses Physik der Hochpolymeren im Rahmen der Fr{ü}hjahrstagung des Arbeitskreises Festk{ö}rperphysik bei der Deutschen Physikalischen Gesellschaft vom 21.--23. M{ä}rz 1973*, E. W. Fischer, F. H. Müller, and H. H. Kausch, Eds. Heidelberg: Steinkopff, 1973, pp. 980–990.

[56] P. V. Joseph, K. Joseph, S. Thomas, C. K. S. Pillai, V. S. Prasad, G. Groeninckx, and M. Sarkissova, "The thermal and crystallisation studies of short sisal fibre reinforced polypropylene composites," *Compos. Part A Appl. Sci. Manuf.*, vol. 34, no. 3, pp. 253–266, 2003.

[57] M. S. Islam, K. L. Pickering, and N. J. Foreman, "Influence of alkali treatment on the interfacial and physico-mechanical properties of industrial hemp fibre reinforced polylactic acid composites," *Compos. Part A Appl. Sci. Manuf.*, vol. 41, no. 5, pp. 596–603, 2010.

[58] L. Avérous, C. Fringant, and L. Moro, "Plasticized starch–cellulose interactions in polysaccharide composites," *Polymer (Guildf).*, vol. 42, no. 15, pp. 6565–6572, 2001.

[59] D. Feng, D. F. Caulfield, and A. R. Sanadi, "Effect of compatibilizer on the structure-property relationships of kenaf-fiber/polypropylene composites," *Polym. Compos.*, vol. 22, no. 4, pp. 506–517, Aug. 2001.

[60] A. Bendahou, H. Kaddami, H. Sautereau, M. Raihane, F. Erchiqui, and A. Dufresne, "Short Palm Tree Fibers Polyolefin Composites: Effect of Filler Content and Coupling Agent on Physical Properties," *Macromol. Mater. Eng.*, vol. 293, no. 2, pp. 140–148, Feb. 2008.